# In vitro electrochemical properties of biodegradable $ZrO_2$-CaO coated MgCa alloy using atmospheric plasma spraying

B. ISTRATE [a], D. MARECI [b], C. MUNTEANU[a*], S. STANCIU[c], D. LUCA[c], C.I. CRIMU[a], E. KAMEL[d]
[a]*Faculty of Mechanical Engineering, The "Gheorghe Asachi" Technical University of Iaşi, Bd. D. Mangeron 6, 700050 Iaşi, Romania*
[b]*"Gheorghe Asachi" Technical University of Iasi, Faculty of Chemical Engineering and Environmental Protection, 73 Prof. dr. doc. D. Mangeron Blvd., 700050, Iasi, Romania*
[c]*Faculty of Materials Science and Engineering, The "Gheorghe Asachi" Technical University of Iaşi, Bd. D. Mangeron 41, 700050 Iaşi, Romania*
[d]*"Dunarea de Jos" Univeristy of Galati, Faculty of Medicine, Dental Medicine Department, Galati*

$ZrO_2$-CaO 95%-5% as a ceramic biomaterial facilitates the osteoconductivity in new bone formation around implant. Surface characterization before and after electrochemical testing was performed used scanning electron microscopy (SEM). $ZrO_2$-CaO coating was performed using a Sulzer Metco 9MCE Atmospheric Plasma Spraying facility. The electrochemical properties of the calcium oxide stabilized zirconium oxide coated and uncoated MgCa sample at the open circuit potential at different immersion time in Ringer's solution were studied by electrochemical impedance spectroscopy (EIS). Equivalent circuit (EC) was used to modeling EIS data, in order to characterize $ZrO_2$-CaO coated and uncoated MgCa surface.

(Received March 18, 2015; accepted June 24, 2015)

*Keywords*: Mg-Ca alloy, $ZrO_2$-CaO-coated, plasma spraying, EIS, SEM

## 1. Introduction

In order to improve the properties of Mg-Ca alloys, in matter of corrosion resistance, surface coatings are quite useful. Compared to the other techniques, atmospheric plasma deposition is a versatile technique that can coat alloy's surface without altering the bulk properties of the biodegradable alloy. In recent years, Mg and its alloys are considered for use as biodegradable implant materials for bone implants [1] as well as for cardiovascular stents [2].

In recent years, researchers have been intensive efforts to study the "biodegradable implants". There are non-toxic implant materials that become resorbed by the human body after a certain period of time. Mg is a important element involved in various metabolic and biological reactions and also stimulates adhesion of osteoblastic cells [3]. Mg-based alloys are potential candidates for biodegradable implants [8-11]. Unfortunately, magnesium has a very high chemical activity with a standard potential of about 1.7 V with respect to a standard hydrogen electrode in an aqueous solution [4]. The high corrosion rate makes the biodegrability process to be faster than the time required to heal the bone [12].

Calcium was selected as an alloying element considering that the degradation products are expected to be non-toxic[13]. The appropiate Ca content in Mg-Ca biodegradable should be in the range of 0.6% Ca [5,6]. Surface modification used to improve the corrosion resistance of metallic biomaterials seems attractive. Piconi et. al. stated that zirconia ($ZrO_2$) cytotoxicity was lower than the one of $TiO_2$ rutile [14]. Zirconia is a ceramic and is evaluated as hard coating. However, hard coatings such as zirconia deposited by plasma spraying are often porous [7].

Recently, Bozzini et al.[15], indicates that zirconia is an appealing material for implants because have a good biocompatibility and oseointegration. Ceramic coatings obtained by atmospheric plasma spraying technique have been used as protective layers for metallic components [16,17]. The disadvantages correlated with atmospheric plasma spraying (APS) of ceramic films are the rapid solidification of the flight particles. An easy approach for determine the modifications of the biomaterials properties are electrochemical tests.

Using electrochemical impedance spectroscopy much more information can be collected than by direct current (DC) electrochemical methods. However, the alternating current (AC) impedance method is particularly useful when monitoring electrochemical change as a function of time [18-21].

The aim of this paper, the degradation characteristics of calcium oxide stabilized zirconia coating by atmospheric plasma sprayed on MgCa alloy as biodegradable biomaterials for biomedical applications will be evaluated using EIS method in Ringer's solution at 37 $^oC$.

## 2. Materials and methods

### 2.1. Materials

Mg-Ca alloy was obtained by melting in a high frequency induction furnace (20 KHz) with controlled atmosphere of Ar, type Enterprise Ultracast (1800ºC). For casting it was used 99.999% Mg metal alloy with pre-alloy of Mg-Ca - 3%Ca. Chemical composition correction was made by repeated casting until final composition of 0.4% Ca(wt.%).

The chemical compositions has been determined by EDX analysis using a scanning electron microscope Quanta 3D (FEI, Hillsboro, OR, USA) – SEM equipped with EDX detector. The above mentioned percentages of alloying elements have been calculated as average of ten values. Two layers, first one thinner, second one thicker, on Mg-Ca alloy by plasma spray system (SPRAYWIZARD-9MCE, Sultzer-Metco, USA) were obtained from bulks samples of $ZrO_2$ produced by Sultzer-Metco, USA. The test $ZrO_2$CaO-coated and uncoated MgCa alloys was placed in a glass corrosion flow cell kit (C145/170, Radiometer, France), which was filled with Ringer's solution.

*Table 1. Deposition parameters for plasma-sprayed coatings*

| | |
|---|---|
| Coating | $ZrO_2$CaO 95-5 |
| Powder Supplier | MTS 8013 |
| Feeding mode | Internal |
| Arc current(A) | 500 |
| Arc voltage(V) | 50 |
| Working gases | Ar, $H_2$ |
| Torch traverse | 1st film- 4 passes<br>2nd fim- 6 passes |
| Spray distance (mm) | 150 |

### 2.2 Coating deposition

The test $ZrO_2$CaO-coated and uncoated MgCa alloys was placed in a glass corrosion flow cell kit (C145/170, Radiometer, France), which was filled with Ringer's solution. A saturated calomel electrode was used as the reference electrode, and a platinum coil as the counter electrode. The potentials in this paper are reported versus the saturated calomel electrode (SCE). The temperature of the electrochemical cell was maintained at 37 ± 1 $^{o}$C.

Electrochemical measurements were performed using a potentiostat model PARSTAT 4000 (Princeton Applied Research, NJ, USA). The instrument was controlled by a personal computer and *VersaStudio* software. Prior to testing, the uncoating electrodes were mechanically abraded using emery paper up to 2000 grit, next polished with 0.3 μm alumina suspension, ultrasonically cleaned in acetone and deionized water, and finally dried in open air.

Electrochemical impedance spectra were measured over a frequency range extending from 100 kHz to 10 mHz using a 10 mV amplitude AC voltage signal. The EIS tests were recorded at the open circuit potential developed by the samples after 1-day, and 1-week of immersion in test solutions. Analysis of the spectra was performed in terms of equivalent circuit (EC) fitting using *ZSimpWin* software.

The surface morphology of $ZrO_2$CaO -coated MgCa alloys after 1-week exposure times Ringer's solution before and after removing corrosion products was assessed using scanning electron microscopy (SEM; Quanta 3D, FEI, Hillsboro, OR, USA). The corrosion products were removed from both alloys in a chromic acid solution, according to ASTM G1-90 (ASTM G1-90, 1999).

## 3. Results and discussions

### 3.1. Structural analysis

The planar and cross-section SEM images of the ZrO2-CaO are shown in Figs. 1 and 2(a-b). Both metallic surfaces covered by $ZrO_2$-CaO exhibited pores and splats. The topography of the ZrO2-CaO can also be observed from the inspection of the SEM images taken from cross-sections through the coated layer (cf. Figs. 1a and 2a).

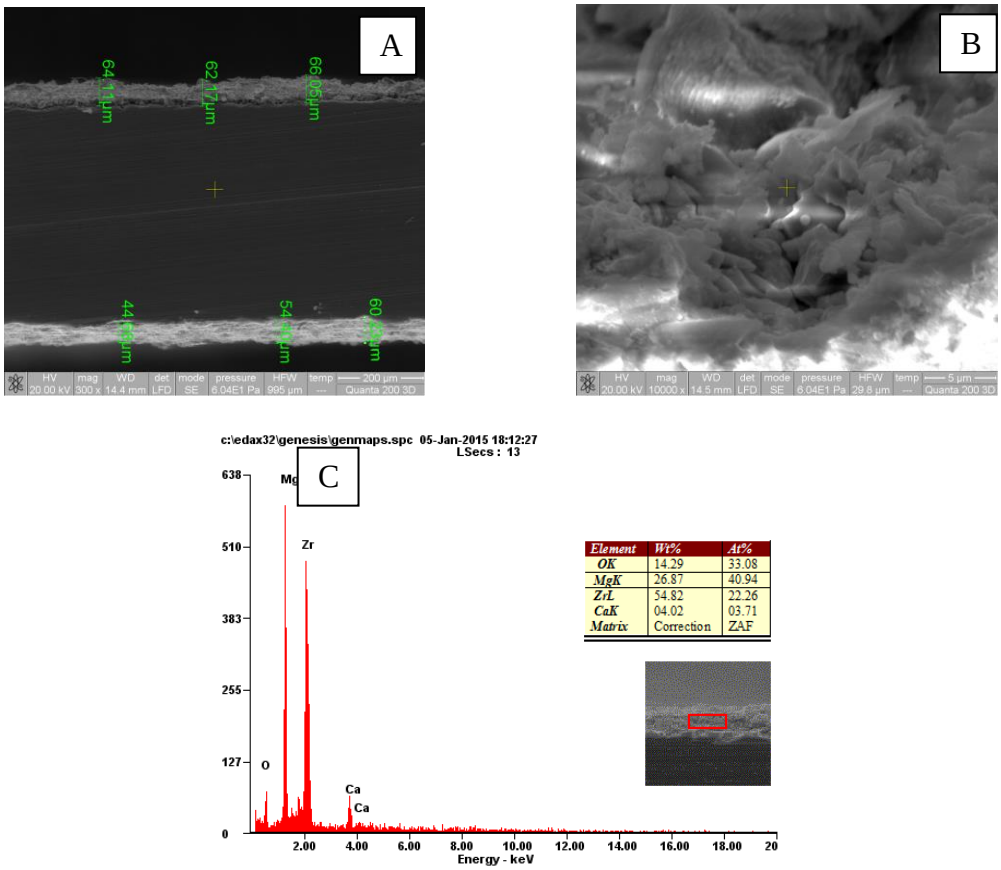


*Fig. 1. Cross-section (A) Planar (B), SEM images of the ZrO2-CaO - coated MgCa alloy and EDX analysis (C) of the $ZrO_2$-CaO -coated MgCa alloy.*

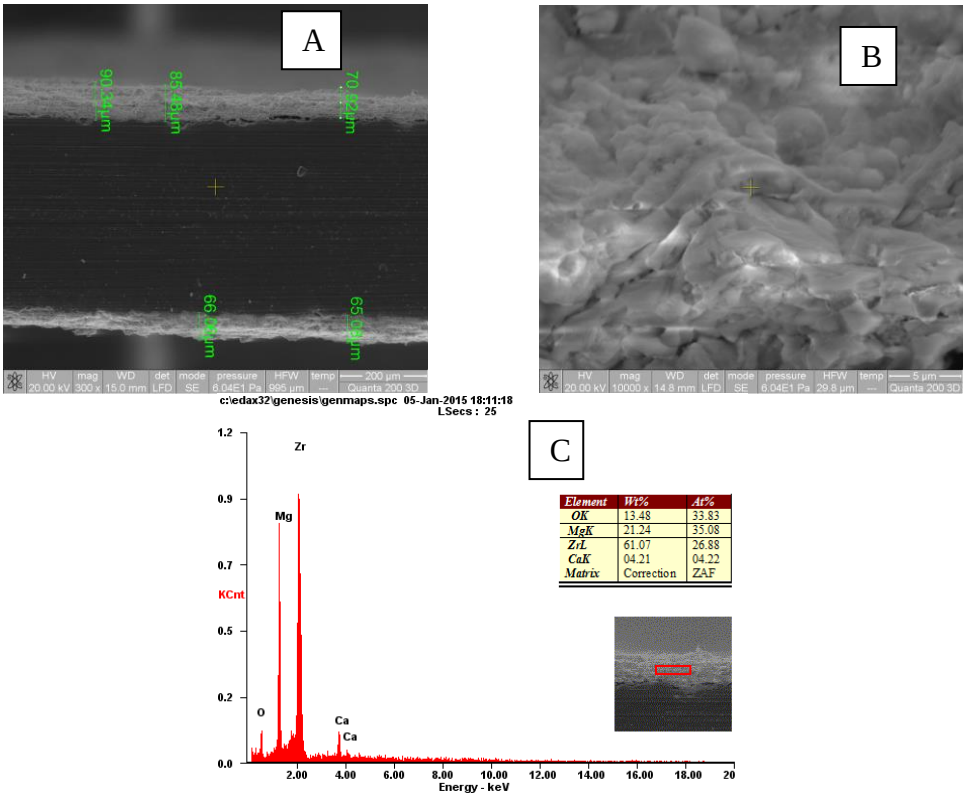


*Fig. 2. Cross-section (A) Planar (B), SEM images of the $ZrO_2$-CaO - coated MgCa alloy and EDX analysis (C) of the $ZrO_2$-CaO -coated MgCa alloy.*

### 3.2. Electrochemical impedance spectroscopy

Measurements of electrochemical impedance have been carried out at the open circuit potential after immersion for both times in Ringer solution, at 37 °C. The measured impedance spectra can be displayed in the form of a complex plane plot, also called Nyquist diagrams, and/or as Bode diagrams. The Nyquist plot displays the impedance data by the complex variables and separated into the real, $Z_{re}$, and the imaginary, $Z_{im}$, parts, expressed in Ω $cm^2$. In the Bode diagram the frequency dependence of the absolute magnitudes of the impedance modulus, $|Z|$, and the phase angle, Φ, are plotted instead. The advantages of this procedure are that the data for all measured frequencies are shown and a wide range of impedance values can be displayed simultaneously. The frequency dependence of $\log|Z|$ and Φ Selected examples of the Nyquist and Bode impedance plots obtained for the coated samples at different exposures in the test electrolyte are shown in figures 3(A-B). Selected examples of the Nyquist and Bode impedance plots obtained for the first coated samples at both exposures in the test electrolyte are shown in figures 4(A-B).

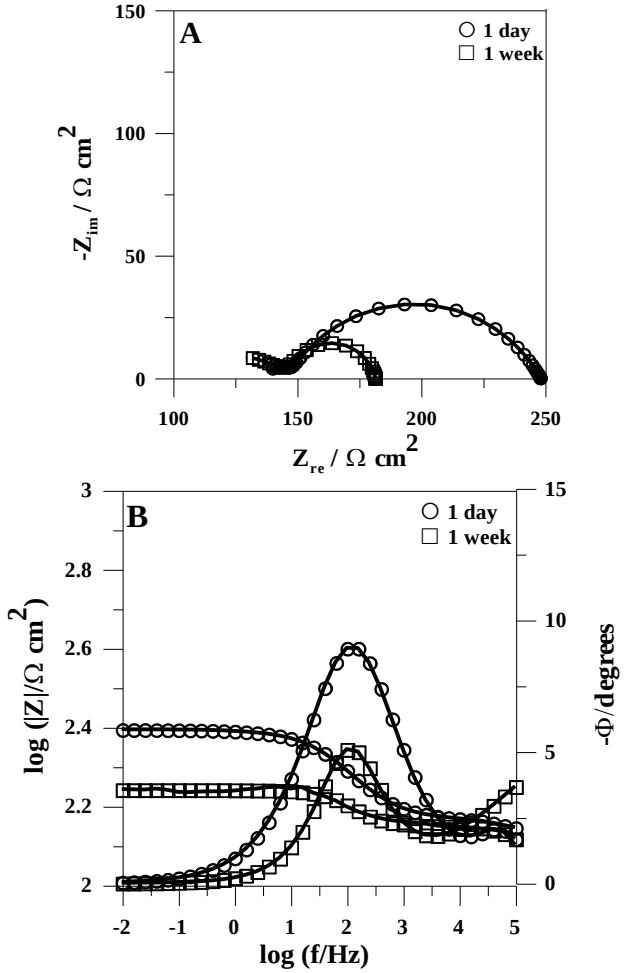


*Fig. 3. Experimental impedance spectra of a MgCa coated with an ZrO2-CaO first film in Ringer's solution at different exposure times as indicated in the graphs. Coating thickness: around 60µm*

Application of the primer coating in one single layer is considered first. When the thin film is considered ($ZrO_2$-CaO coating, around 60µm thick), the formation of a poorly protective film on MgCa alloy is clearly evidenced from the observation of both Bode-modulus and Bode-phase diagrams at both times. Low impedance modulus values in the order of $10^2$ Ω $cm^2$ were measured even at the earliest exposures, whereas the response of the system must be described as resistive over all the frequency range.

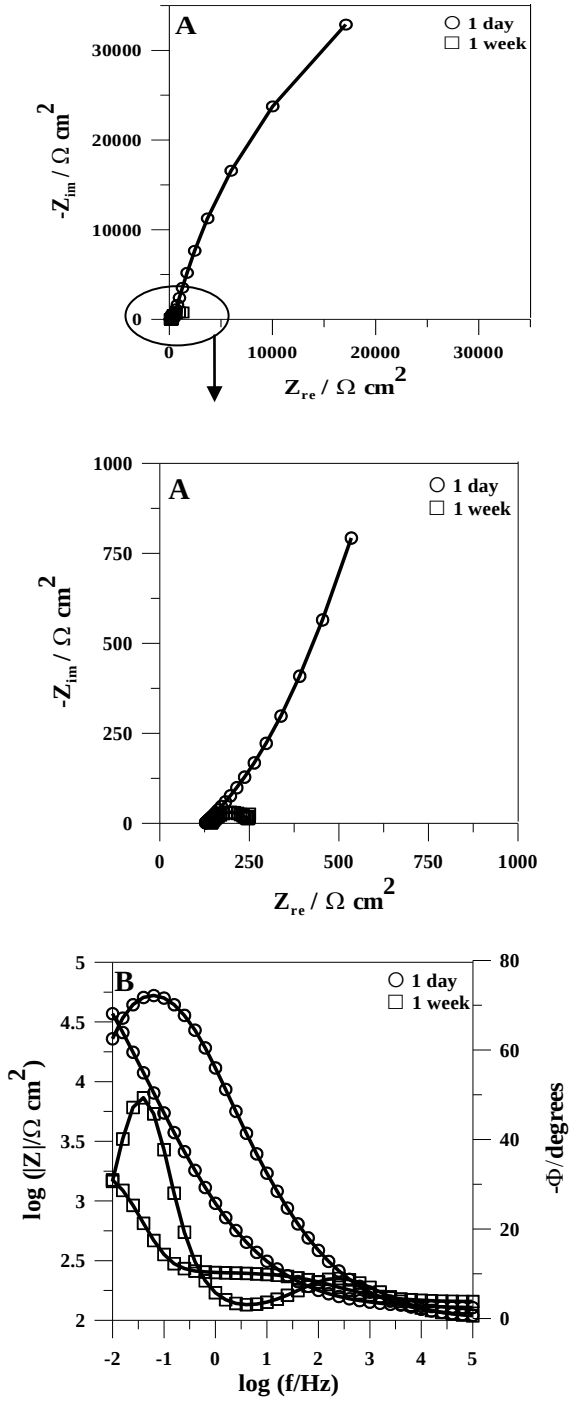


*Fig. 4. Experimental impedance spectra of a MgCa coated with an ZrCa second film in Ringer's solution at different exposure times as indicated in the graphs. Coating thickness: around 75µm*

A better situation was observed with the second thicker coating applied on MgCa alloy (ZrO2-CaO coating, around 75 μm thick), shortly after immersion in the test electrolyte. Initial modulus values in the low frequency range of the impedance spectra amounting ca. $10^4$ Ω cm$^2$ were observed this time (cf. Fig. 4), and even a small frequency range with phase angles in excess of 10 degrees could be observed in the Bode-phase diagrams at the high frequency limit. Despite these observations, phase angles were always smaller than 75 degrees, which would be an indication of a dielectric behavior.

Analysis of Bode spectra in terms of an equivalent circuit (EC) allowed the values of the impedance parameters. The EIS spectrum measured for uncoated MgCa alloy in Ringer's solution, at 37 $^o$C, could be satisfactorily fitted with the model presented in Fig. 4. The experimental data show good fitting and an error smaller than 5%. Table 1 shows the results of the fits.

Constant phase elements (CPE) were used instead of pure capacitances because of the non-ideal capacitive response due to the distributed relaxation feature of the passive oxide layer thermal generated. The impedance representation of CPE is given by equation (1):

$$Z_{(CPE} = \frac{1}{Y_0(j\omega)^n} \qquad (1)$$

where ω is the angular frequency and $Y_0$ is a constant, and the value of the exponent n indicates the deviation from ideal capacitive behaviour (e.g., when n = 1).

$R_{sol}$ is the resistance of solution occurring between the sample and the reference electrode. This parameter has a value around 80 ± 5 Ω cm$^2$ in Ringer's solution, and is not listed in Table 2.

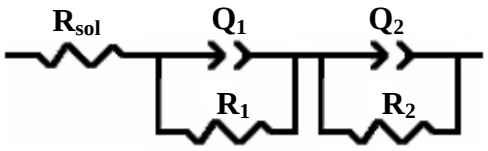


*Fig.5. Equivalent circuits (ECs) used to fit the impedance data*

The $R_1$ and $Q_1$ parameters describe the processes occurring at electrolyte/coating layer. $R_1$ is the charge transfer resistance associated with the penetration of the electrolyte trough the pores or pinholes existing in the coated layer and $Q_1$ correspond to capacitance of the coating layer. Such behavior is typical for a metallic material covered with a porous film, which is exposed to an electrolytic environment [22].

*Table 2. Electrochemical parameters obtained from EIS spectra using the selected EC for the $ZrO_2$-CaO coated MgCa alloy after different immersion time in Ringer's solution, at 37 $^o$C.*

| Samples | Immersion time | $10^4 Q_1$, S/cm$^{-2}$s$^n$ | $n_1$ | $R_1$/ Ω cm$^2$ | $10^4 Q_2$/ S cm$^{-2}$ s$^n$ | $n_2$ | $R_2$/ Ω cm$^2$ |
|---|---|---|---|---|---|---|---|
| First layer coated MgCa alloy | 1-day | 1.1 | 0.80 | 159 | 0.9 | 0.79 | 240 |
| | 1-week | 1.4 | 0.80 | 26 | 1.1 | 0.78 | 165 |
| Second layer coated MgCa alloy | 1-day | 1.1 | 0.81 | 67 | 0.3 | 0.81 | 3750 |
| | 1-week | 1.1 | 0.80 | 58 | 0.5 | 0.80 | 1530 |

Corrosion may occur at pores as the result of the metal being directly exposed to the aggressive attack of the electrolyte. The decrease of $R_1$ and $R_2$ as immersion time increases imply that increased number of opening pinholes and pores the coating layer became more conductive.

The formation of $Mg(OH)_2$ substrate layer is accompanied by the intense hydrogen evaluation reaction seen by visual inspection [23].

As a result, the formed $Mg(OH)_2$ layer cannot provide effective protection to the Mg and is strongly attacked in the presence of chloride anions to produce soluble compounds [24].

### 3.3 SEM analysis of corroded surfaces

The surface topography of first layer $ZrO_2$-CaO-coated MgCa alloy samples after 1 week immersion times in Ringer's solution were examined by scanning electron microscopy (SEM) and are displayed in Fig. 6A. The ZrO2CaO-coated MgCa alloy is covered by relatively massive corrosion products containing relatively large clusters of crystals.

After 1 week immersion time in Ringer's solution, the surface layer of the corrosion products it is attacked of chloride ions. EDX analysis (Fig. 6B) proved the existence of chlorides in the corrosion product layer.

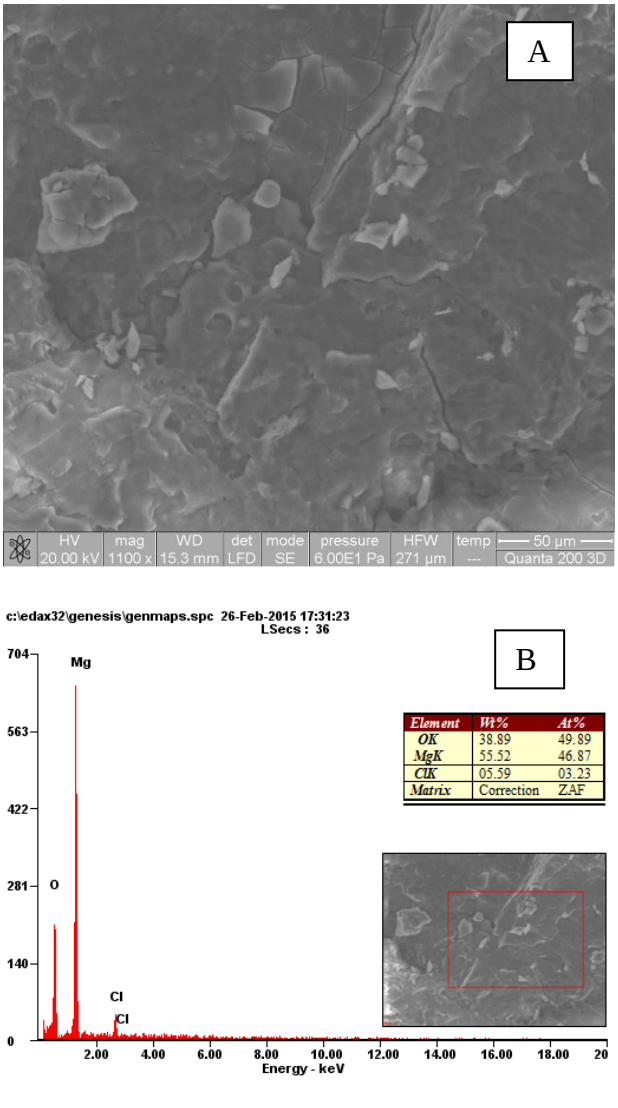


*Fig. 6. Corroded SEM (A) morphologies of ZrO2CaO-coated MgCa alloy with corrosion products removed after one-week immersion in Ringer's solution, and (B) EDX spectra of area (A).*

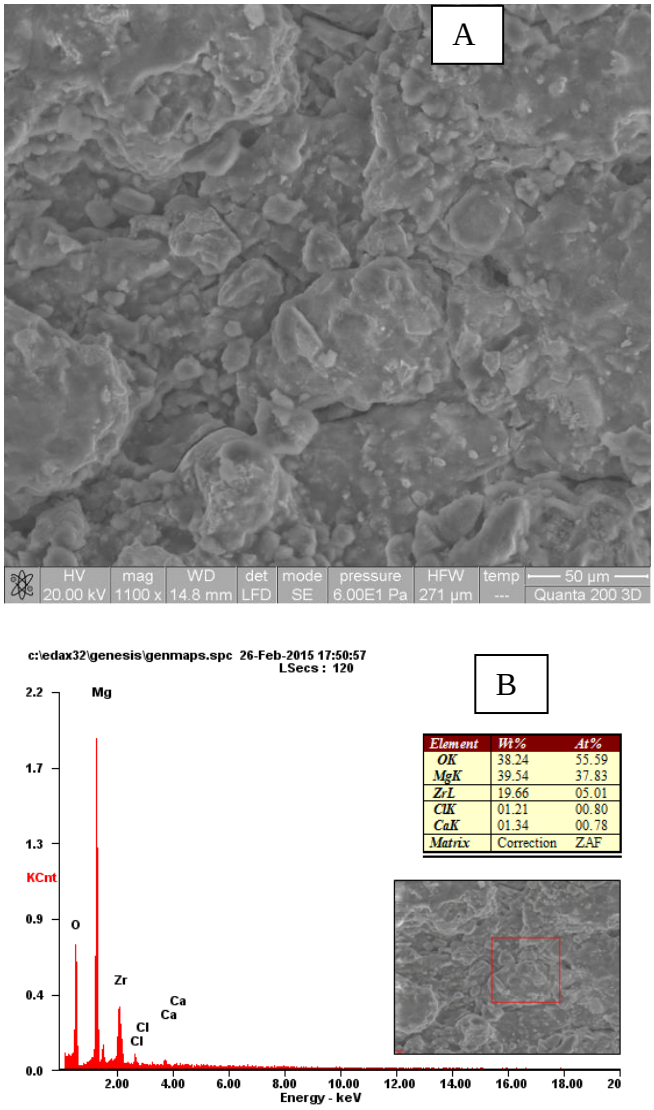


*Fig. 7. Corroded SEM (A) morphologies of $ZrO_2$CaO-coated MgCa alloy with corrosion products removed after one-week immersion in Ringer's solution, and (B) EDX spectra of area (A).*

Fig. 7A shows the corroded surface morphologies of second layer $ZrO_2$-CaO-coated MgCa alloy. The EDX analyses (Figure 7B) indicate the presence of Zr on the corroded surface of $ZrO_2$-coated MgCa alloy.

## 4. Conclusions

The electrochemical impedance experiments proved to be a good test for studying the resistance of the $ZrO_2$-CaO coatings deposited on Mg-Ca alloy during exposure in Ringer's solution.

Because the coatings are porous direct paths between the corrosive environment and the base material can eventually formed. The impedance data showed significant differences that could be related to variations in time immersion, porosity, and thickness of the coating. Due it's thicker, compact and dense layer, second layer impedance show a better corrosion resistance than the first layer. Optimization of the plasma deposition in terms of powder flow rate, spray distance and layer thickness will result lower degradation rates for magnesium alloys.

## References


[1] M.P. Staiger, A.M. Pietak, J. Huadmai, G. Dias, Biomaterials **27**, 1728 (2006).

[2] B. Heublein, R. Rohde, V. Kaese, M. Niemeyer, W. Hartung, A. Haverich, Heart **89,** 651 (2003).

[3] A. Hartwig, Mutat. Res. Fundam. Mole. Mech. Mutagen. **475**, 113 (2001).

[4] G. Song, A. Atrens, Adv. Eng. Mater. **5** 837 (2003).

[5] Z. Li, X. Gu, S. Lou, Y. Zheng, Biomaterials **29,** 1329 (2008).

[6] Y. Wan, G. Xiong, H. Luo, F. He, Y. Huang, X. Zhou, Materials & Design **29,** 2034 (2008).

[7] S. Deville, J. Chevalier, G. Fantozzi, J. F. Bartolome, J. Requena, J. S. Moya, R. Torrecillas, L. A. Diaz, Key Eng. Mater. **264-268**, 2013 (2004).

[8] D. Tie, F. Feyerabend, N. Hort, D. Hoeche, K. U. Kainer, R. Willumeit, W. D. Mueller, Materials and Corrosion **65,** 569 (2014).

[9] J.-S. Zhang, D. Wang, W.-B. Zhang, H.-X. Pei, Z.-Y. You, C.-X. Xu, W.-L. Cheng, Materials and Corrosion, DOI: 10.1002/maco.201407696.

[10] T. Li, H. Zhang, Y. He, X. Wang, Materials and Corrosi*on*, DOI: 10.1002/maco.201307528

[11] P. Rosemann, J. Schmidt, A. Heyn, Materials and Corrosion, **64,** 714 (2013).

[12] Z.J. Li, X.N. Gu, S.Q. Lou, Y. F. Zheng, Biomaterials; **29,** 1329 (2008).

[13] J.Z. Ilich, J.E. Kerstetter, J. Am. Coll. Nutr., **12,** 715 (2000).

[14] C. Piconi, G. Maccauro, Biomaterials, **20**, 1 (1999).

[15] B. Bozzini, P. Carlino, C. Mele, Journal of Materials Science: Materials in Medicine **22**, 193 (2011).

[16] M.F. Morks, Y. Gao, N.F. Fahim, F.U. Yingqing, Materials Letters, **60**, 1049 (2006).

[17] M.F. Morks, Y. Gao, N.F. Fahim, F.U. Yingqing, M.A. Shoeib, Surface & Coating Technology, **199**, 66-71. (2005),

[18] D. Mareci, R. Chelariu, G. Ciurescu, D. Sutiman, D. M. Gordin, T. Gloriant, J. Optoelectron. Adv. Mater. **12**, 1590 (2010).

[19] D. Mareci, R. Chelariu, I. Dan, D. M. Gordin, T. Gloriant, J. Mater. Sci.-Mater. Med. **21**, 2907 (2010).

[20] D. Mareci, R. Chelariu, G. Bolat, A. Cailean, D. Sutiman, J. Optoelectron. Adv. Mater. **14**, 112 (2012).

[21] R. Chelariu, G. Bolat, J. Izquierdo, D. Mareci, D. M. Gordin, T. Gloriant, R. M. Souto, Electrochim. Acta **137**, 280 (2014).

[22] C. Papatoiu , R. Chelariu, G. Bolat, C. Munteanu , D. Mareci, J. Optoelectron. Adv. Mater. **16**, 1093 (2014).

[23] J. Chen, J.Q. Wang, E.H. Han, W. Ke, Electrochem. Commun. **10**, 577 (2008).

[24] X. Liu, D. Shan, Y. Song, R. Chen, E. Han, Electrochim. Acta **56**, 2582 (2011).


*Corresponding author: cornelmun@gmail.com